ELSEVIER

Colloids and Surfaces A: Physicochem. Eng. Aspects 265 (2005) 73–80

COLLOIDS AND SURFACES A

www.elsevier.com/locate/colsurfa

FT-IR–ATR as a tool to probe photocatalytic interfaces

Paula Z. Araujo [a], Cecilia B. Mendive [a,b], Luis A. García Rodenas [a], Pedro J. Morando [a,c], Alberto E. Regazzoni [a,c], Miguel A. Blesa [a,c,*], Detlef Bahnemann [b]

[a] *Unidad de Actividad Química, Centro Atómico Constituyentes, Comisión Nacional de Energía Atómica, Avenida General Paz 1499, 1650 San Martín, Provincia de Buenos Aires, Argentina*

[b] *Institut für Technische Chemie, Hannover Universität, Callinstrasse 3 (30167) Hannover, Germany*

[c] *Universidad Nacional de San Martín, San Martín, Provincia de Buenos Aires, Argentina*

Received 17 June 2004; received in revised form 27 September 2004; accepted 27 October 2004
Available online 9 June 2005

Abstract

The catalytic photo-oxidation on TiO_2 (Degussa P-25) of oxalic acid at pH 3.7 and of catechol at pH 6.2 has been studied by in situ ATR–FT-IR. In the case of catechol, both FT-IR and HPLC demonstrate the formation of an intermediate, the accumulation of carbonate, and the depletion of the ligand on the illuminated surface. Ligand depletion is also demonstrated by the spectral evolution of adsorbed oxalate; the data in the case also suggest that different surface complexes may inter-convert directly on the surface. These findings illustrate the potentiality of in situ ATR–FT-IR to follow the evolution of the catalytic surface. It is also clearly demonstrated that under our experimental conditions, the photolytic oxidation of the adsorbed ligands is fast as compared with the rate of exchange with the bulk. In terms of simple mechanistic considerations, the systems behave as expected for low degrees of coverage, determined by fast surface reactions, $k_2\{h^+\} \gg k_{-1}$, where k_{-1} is the rate constant for hole trapping by the adsorbed ligand, k_{-1} the rate constant for ligand desorption, and $\{h^+\}$ is the effective hole concentration, determined by the intensity of light. The rate law then turns out to be $R = k_1 N_S[HL]$, where R is the reaction rate, k_1 the adsorption rate constant, N_S the surface site density, and [HL] is the bulk ligand concentration.

Keywords: Photocatalysis; Gallic acid; Catechol; Intermediates; Surface complexes; FT-IR/ATR

1. Introduction

FT-IR spectroscopy has been used extensively to characterize the adsorption of inorganic and organic anions onto metal oxide particles immersed in water [1–7]. Both structural and thermodynamic information has been accrued using this technique. The formation of surface complexes has been demonstrated by the position of certain vibrations, such as the C=O stretching in carboxylate groups of the ligand, and Langmuir-type stability constants have been derived through the analysis of the spectral changes attending variations in the concentration of the ligand in the aqueous solution, at constant pH. The analysis of these spectral changes using singular value decomposition (SVD) procedures has also permitted to demonstrate the formation of more than one surface species.

Earlier [6], we have shown that in simple cases ATR–FT-IR can be used to probe the attainment of surface speciation equilibrium when competitive chemisorption takes place. Specifically, the exchange of oxalate for salicylate (and vice versa) onto titanium dioxide was demonstrated to follow the predictions of simple equilibrium calculations, based on the stability constants obtained from systems that contain each ligand alone.

The use of FT-IR to characterize interfaces under non-equilibrium conditions has been much more limited. Recently, Kesselman-Truttmann and Hug [8] demonstrated that the photodegradation of 4,4′-bis(2-sulfostyryl)biphenyl can be characterized by following the ATR–FT-IR spectral evolution. Here, we show that ATR–FT-IR also sheds light on the dynamics of mass transfer across the TiO_2/aqueous

* Corresponding author.
E-mail address: miblesa@cnea.gov.ar (M.A. Blesa).

0927-7757/$ – see front matter © 2005 Elsevier B.V. All rights reserved.
doi:10.1016/j.colsurfa.2004.10.137

solution interface, when the interfacial species undergo chemical changes caused by light-induced heterogeneous oxidation. To illustrate this, we have studied the spectral evolution of the surface of TiO_2 films in contact with solutions containing oxalic acid or catechol during UV illumination.

The mechanisms of heterogeneous photo-catalytic oxidation reactions may vary widely, and may involve direct hole trapping by specific surface complexes, or the mediation of surface >OH$^\bullet$ radicals that oxidize the organic compounds when released from the surface [9–12]. In the case of organic anions with a large affinity for the surface, such as oxalate and catecholate [13,14] the former mechanism is very likely to be involved [15], even if a parallel path via >OH$^\bullet$ also contributes to the overall rate.

2. Materials and methods

2.1. Materials

Titanium dioxide was Degussa P-25. It is composed mainly of anatase, with a rutile content of ca. 20%. The modal particle size was ca. 30 nm, and its BET specific area was 51.4 $m^2\,g^{-1}$. Degussa P-25 was used without further purification. All other reagents were analytical grade and used as received. All solutions were prepared with deionized water from an E-pure apparatus (conductance = 18.2 $M\Omega\,cm^{-1}$).

2.2. Methods

Dark adsorption experiments were performed as described earlier [5]. Typically, successive TiO_2 layers were deposited onto the ATR crystal by placing 0.15–0.35 cm^3 of a TiO_2 suspension (4–20 g dm^{-3}) and evaporating to dryness at room temperature. The calculated final thickness of the layers was in the order of 1–2 μm. Prior to use, the TiO_2 film was rinsed with water to eliminate loosely adhered particles. Fresh adsorbate solutions of predetermined concentration, pH and ionic strength (10^{-2} M KCl) was placed in contact with the TiO_2 film and the FT-IR spectrum was recorded until no further changes were detected; solution volumes were 3 ml for oxalate and 1.8 ml for catechol. Equilibration times were in the order of 30 min. The spectra were collected in either a Nicolet Magna 560 or a Bomem MB 122 instrument, equipped with a liquid N_2 cooled MCT-A detector and a Spectra Tech ZnSe–ATR unit (area = 10 mm × 72 mm) with an incident angle of 45°; the total number of reflections was 11. Spectra were taken with 200 or 250 scans at 4 cm^{-1} resolution, the background was subtracted and baseline correction was made due to instrumental instabilities.

FT-IR spectra of the solid adsorbates, and of their aqueous solution (FT-IR–ATR) were obtained for comparative purposes. The signal due to dissolved catechol was negligible when the concentration was below 10^{-3} M, and this concentration was set as an upper limit; for oxalate, this limit was ca. 5×10^{-3} M.

Photo-oxidation experiments were performed once dark adsorption equilibrium had been attained, by exposing the film to UV light. A 15 W lamp with a maximum wavelength of 365 nm was used. Light intensity was adjusted by setting the appropriate distance from the light source to the sample, and measured either by means of a UV-meter or actinometry. ATR–FT-IR spectra were then collected either under continuous irradiation (for oxalate) or after pre-fixed irradiation times (for catechol). In the latter case, no significant spectral changes took place during the post-irradiation dead-time (less than 2 min), as it was assessed by independent kinetic adsorption measurements; in the case of oxalate, on the other hand, the faster adsorption renders this procedure inadequate. Photo-oxidation and dark adsorption experiments were performed under stagnant conditions.

Catechol photodegradation was also followed by measuring the ligand concentration in the remnant solutions. Catechol concentration was determined by HPLC in an equipment fitted with an Alltech 301 HPLC-pump, a UV1000 Spectra System detector, a 200 μl injection loop, and a 79427 PRP-1 C18 column. The flow rate was 1.5 $cm^3\,min^{-1}$, and the detection wavelength was 275 nm. An acetic acid–water–methanol solution was used as eluent. The retention time of catechol was 18.6 min.

Adsorption and TiO_2 catalyzed photo-oxidation were studied at several pH values; the lower limit was set to protect the integrity of the ATR crystal, and the upper one to avoid catechol decomposition. Here, we shall report the results from experiments carried out at pH 6.2 ± 0.2 (for catechol) and pH 3.7 ± 0.3 (for oxalate).

3. Results

Fig. 1a shows the ATR–FT-IR spectra obtained in the dark, when oxalic acid solutions of increasing concentrations and pH 3.7 are equilibrated with the TiO_2 film. SVD analysis demonstrates the presence of three surface species. Their spectra, which are shown in Fig. 1b, can be solved assuming that each adsorption equilibria is described by a Langmuir equation. The best fitting Langmuir constants are given in Table 1. It also includes band assignments. Analysis of the IR band shifts suggests that the three surface complexes are as shown in Fig. 1c [5–7].

Fig. 2a shows the ATR–FT-IR spectra of the TiO_2 film in contact with catechol solutions, at pH 6.2. In this case, SVD analysis identifies only one spectral component. Most of the signal is well modeled by a single Langmuir type isotherm. However, a second contribution, which accounts for less than 5% and increasing linearly with total concentration, improves the fit. This behavior agrees with that previously reported on 4-chlorocatechol [16]. Table 1 includes the Langmuir-type constant for catechol adsorption, and band assignments.

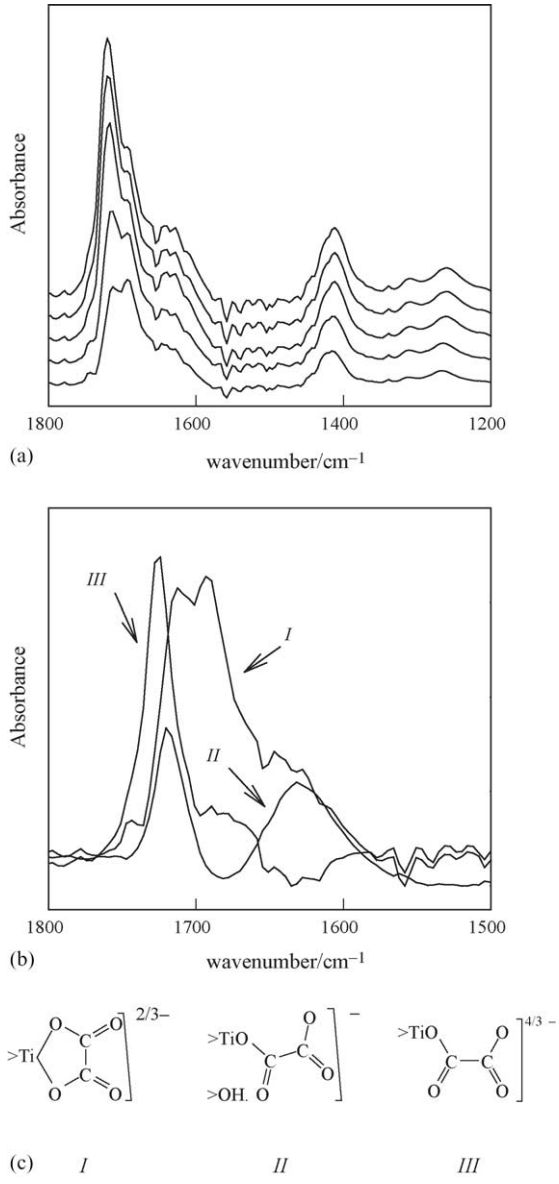

Fig. 1. (a) ATR–FT-IR spectra of a TiO_2 film in contact with solutions of increasing oxalic acid concentration in the dark. From bottom to top: 1.0×10^{-6}, 1.4×10^{-5}, 2.1×10^{-4}, 6.5×10^{-4}, and 1.3×10^{-3} M; pH 3.7. (b) Contribution of the oxalato surface complexes to the overall absorbance in the 1800–1500 cm^{-1} spectral region assessed by SVD (see text). (c) Postulated surface species (from Ref. [5]).

Fig. 2b shows the possible structures of the surface complex, as diagnosed from band shifts.

Figs. 3 and 4 show the time evolution under irradiation of the ATR–FT-IR spectra of the surface complexes formed upon oxalate chemisorption, for two different lamp outputs, 0.6 and 1.0 mW cm^{-2}, respectively. Comparison of Figs. 3 and 4 with Fig. 1, shows some differences in the spectra in the dark, that should be attributed to the different experimental conditions under which the spectra were recorded. These differences are mainly associated with the noisy region of water absorption, and we shall not discuss these differences

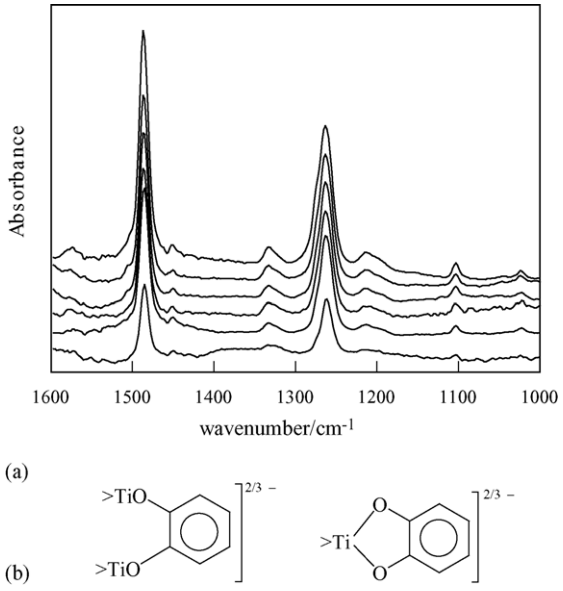

Fig. 2. (a) ATR–FT-IR spectra of catechol adsorbed onto TiO_2 in the dark for increasing catechol concentrations. From bottom to top: 1.1×10^{-5}, 5.0×10^{-5}, 7.5×10^{-5}, 1.0×10^{-4}, 2.0×10^{-4}, and 5.0×10^{-4} M; pH 6.2. (b) Postulated surface species.

any further.[1] More important for us is to notice that the effect of irradiation mimics the effect of decreasing bulk oxalate concentration, and to point the marked change of the relative intensities of the bands at 1720 and 1692 cm^{-1}. These observations indicate that photolysis of the surface complexes is accompanied not only by an overall decrease in the degree of coverage, but also by changes in the speciation of adsorbed oxalate.

A very important observation is that the intensity of the signal, as well as the intensity ratio of the peaks at 1720 and 1692 cm^{-1}, rise back when the system is left in the dark after irradiation. These changes (not shown) indicate an increase in the effective surface concentration of oxalate, hence a departure from adsorption equilibrium under light.[2]

Fig. 5 shows the time evolution of the integrated intensity of the spectral region between 1793 and 1682 cm^{-1} that spans bands due to the various surface complexes. For our purposes, Fig. 5 shows that the kinetic profiles are not simple exponential or linear lines, as would correspond to orders 1 and 0, respectively, on the overall surface concentration of oxalate. This finding is not surprising, because the evolution of the spectral area responds to both the changes in the bulk oxalate concentration (in an undefined way), and to the changes in

[1] Note however that Hug (Hug, private communication) has found that the spectra of oxalate onto rutile and onto anatase are not identical, and the spectra on Degussa P-25 might be sensitive to the actual content of each phase.

[2] Earlier (see Ref. [17]), we had interpreted the changes in the intensity of the two main peaks as indicative of overall equilibrium between surface and bulk solutions, even under light. The more precise information gathered here does not support this conclusion.

Table 1
Langmuir conditional stability constants and band assignments for the different surface complexes formed by adsorption of oxalate and catechol onto TiO_2 at 25 °C

Ligand		Surface complex			Assignment
		I	II	III	
Oxalate[a]	log(K_L/M)	6.38	4.48	3.48	
		1712; 1692	1719	1726; ∼1680b	ν(C═O)
			1631		$\nu_a(CO_2^-)$
		1415	1405	1409b	ν(C─O) + ν(C─C)
		1310w	1305w	1308vw	$\nu_s(CO_2^-)$
		1268w	1252w	1254w	ν(C─O) + δ(O─C═O)
Catechol[b]	log(K_L/M)	4.66	–	–	
		1486			ν(C─C)
		1450vw			ν(C═C)
		1332w			
		1263			ν(C─O)
		1215w; 1105w			δ(C─H)

b: broad; w: weak; vw: very weak.
[a] pH 3.7.
[b] pH 6.2.

speciation. Fig. 5 permits to assess qualitatively the influence of light intensity. In the early stages (initial rates), the rate of decrease is proportional to $I^{0.8}$ at [ox] = 2×10^{-3} M, and to $I^{0.45}$ at [ox] = 6.5×10^{-4} M. In latter stages, the influence of light intensity decrease substantially, the exponents being 0.35 and 0.1, respectively.

Fig. 6 shows the time evolution of the spectra of adsorbed catechol at pH 6.2; the arrows indicate the direction of evolution of the main bands. Together with the decrease of the bands at 1486 and 1263 cm^{-1}, there is an obvious increase of a broad band centered at around 1408–1414 cm^{-1}. The strong band of adsorbed oxalate in this region precludes the possible detection of a similar spectral feature in Figs. 3 and 4. In this case, increasing absorbance is seen at around 1610 cm^{-1} (Figs. 3a and 4a); a similar feature seems to appear in the catechol system.

Complementary results, obtained by measuring residual catechol concentration by HPLC, show that the kinetics follows a first order behavior (Fig. 7). The data in Fig. 7 were corrected to take into account the contribution from the direct photolysis of unadsorbed catechol. Additionally, HPLC permitted to detect the build up of a reaction product characterized by an elution time of 14.4 min, as shown in Fig. 8. A careful analysis of the time evolution of the FT-IR bands intensity also supports this idea; Fig. 8 also includes spectral data, as described and analyzed below.

4. Discussion

The main two issues requiring analysis are: (i) the possible accumulation of intermediates and of reaction products, such as carbonate in the surface and (ii) the relative values of the rates of photo-oxidation and of mass transfer (adsorption–desorption) [18].

4.1. Accumulation of intermediates and reaction products in the surface

In the case of oxalate heterogeneous photolytic oxidation, no intermediates are expected to be formed. The product formed upon hole capture, the radical anion $C_2O_4^{\bullet -}$, rapidly injects an electron into the conduction band of TiO_2, yielding 2 CO_2 [11,13,19]. The possible formation of carbonato surface species, upon adsorption of the final oxidation product, can not be excluded, eventhough the measurements were performed at pH values that prevent carbonate adsorption; photo-oxidation produces a decrease in the acidity, thus the local pH might be high enough to allow for carbonate retention. Carbonate adsorption reveals itself in the 1700–1000 cm^{-1} spectral region, showing main bands at 1660–1630 cm^{-1} [20], and at 1550, 1430 and 1290 cm^{-1} [21]. This region, however, is optically opaque due to the strong absorption of the oxalate surface complexes. Nevertheless, the broad feature at ca. 1610 cm^{-1} (Figs. 3a and 4a) might contain a contribution from adsorbed carbonate.

Retention of carbonate is more clearly seen in the case of catechol photo-oxidation, which eventually leads to complete mineralization. The presence of adsorbed carbonate is denoted by the band at 1420–1410 cm^{-1} (Fig. 6);[3] at wavenumbers larger than 1600 cm^{-1}, the spectra become too erratic as to disclose absorption bands. In this case, the pH is also compatible with carbonate fixation on the surface.

ATR–FT-IR also gives evidence of the formation of at least one intermediate during catechol photo-oxidation. Fig. 9 shows the time evolution of the intensity of the 1486 and 1263 cm^{-1} bands observed in the spectrum of adsorbed cate-

[3] As pointed out by an anonymous reviewer, the spectra do not rule out the possible presence of oxalate that might form as an intermediate during the course of catechol mineralization.

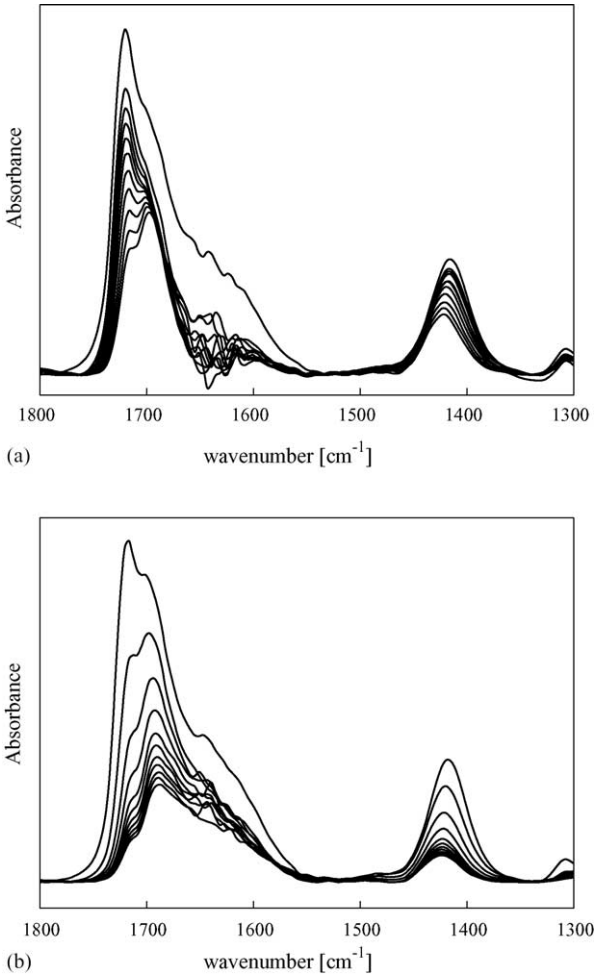

Fig. 3. Time evolution of the ATR–FT-IR spectra of oxalate onto TiO_2 under UV-light irradiation for 2.0×10^{-3} M (a) and 6.5×10^{-4} M (b) adsorbate initial concentration; pH 3.7; light intensity 0.6 mW cm^{-2}. The spectrum in bold line corresponds to equilibrated dark adsorption, for the following descending spectra the time axis is read downwards; spectra were recorded successively at 3.56 min intervals.

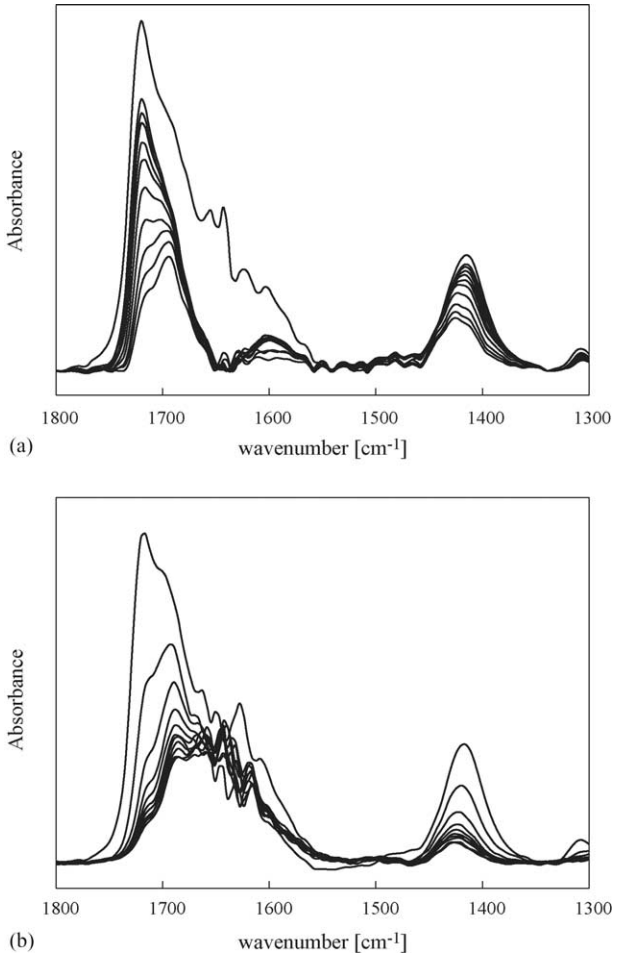

Fig. 4. Time evolution of the ATR–FT-IR spectra of oxalate onto TiO_2 under UV-light irradiation for 2.0×10^{-3} M (a) and 6.5×10^{-4} M (b) adsorbate initial concentration; pH 3.7; light intensity 1.0 mW cm^{-2}. The spectrum in bold line corresponds to equilibrated dark adsorption, for the following descending spectra the time axis is read downwards; spectra were recorded successively at 3.56 min intervals.

chol. It can be seen that the intensity at 1486 cm^{-1} decreases faster, suggesting a contribution from another species to the peak at 1263 cm^{-1}. In order to compare with the information obtained by conventional HPLC measurements, it is assumed that the deviation of the slopes in both curves in Fig. 9 can be attributed to an intermediate. This contribution is given, in absorbance units, by Eq. (1), where the superscript int identifies the intermediate, and the superscript 0 denotes $t = 0$.

$$^{\text{int}}A_{1263} = A_{1263} - \frac{A^0_{1263}A_{1486}}{A^0_{1486}} \quad (1)$$

The data plotted in Fig. 8 were calculated using Eq. (1). It can be seen that there is a rough parallelism with the information obtained by HPLC.

The nature the intermediates of catechol photo-oxidation has been discussed in the literature [22–24]. Formation of 1,2,3-trihydroxybenzene and 1,2,4-trihydroxybenzene has been documented. These compounds, which are more polar than catechol and elute at shorter times, present also large affinity for the TiO_2 surface. However, they compete unfavorably with catechol, and contribute to the ATR–FT-IR signal modestly. Adsorption, nevertheless, may account for the mismatch observed at long reaction times (Fig. 8).

4.2. Kinetic regimes

The spectral data demonstrate that the dark equilibrium condition between bulk and surface for oxalate adsorption, is not maintained during illumination. The observed surface depletion is accompanied with further adsorption when the light is shut off. The lack of a simple kinetic behavior (e.g., simple first or zero order on adsorbed oxalate, or a constant influence of light intensity along a wide surface concentration range), indicates that the surface is rapidly depleted of oxalate in the early stages, until a second kinetic regime is reached, in

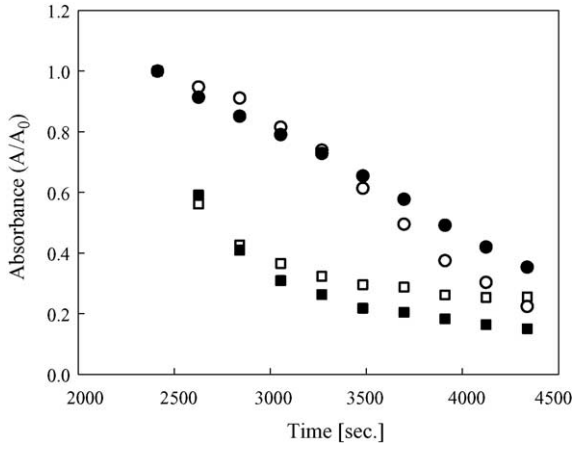

Fig. 5. Time profiles of the absorbance integrated between 1793 and 1682 cm^{-1}: (●) initial oxalic acid concentration: 2.0×10^{-3} M; light intensity: 0.6 mW cm^{-2}; (◯) initial oxalic acid concentration: 2.0×10^{-3} M; light intensity: 1.0 mW cm^{-2}; (■) initial oxalic acid concentration: 6.5×10^{-4} M; light intensity: 0.6 mW cm^{-2}; (□) initial oxalic acid concentration: 6.5×10^{-4} M; light intensity: 1.0 mW cm^{-2}; pH 3.7.

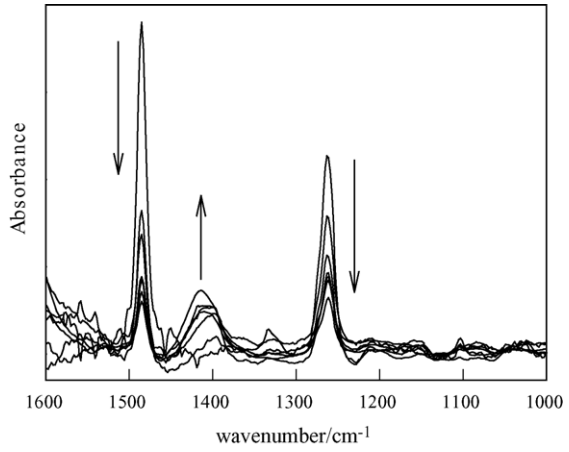

Fig. 6. Time evolution of the ATR–FT-IR spectra of catechol onto TiO_2 under UV-light irradiation; the spectra correspond to 0, 7, 10, 15, 20, 30 and 40 min irradiation; the arrows indicate the direction of evolution of the main bands; light intensity: 1.95×10^{-4} E cm^{-2}; pH 6.2.

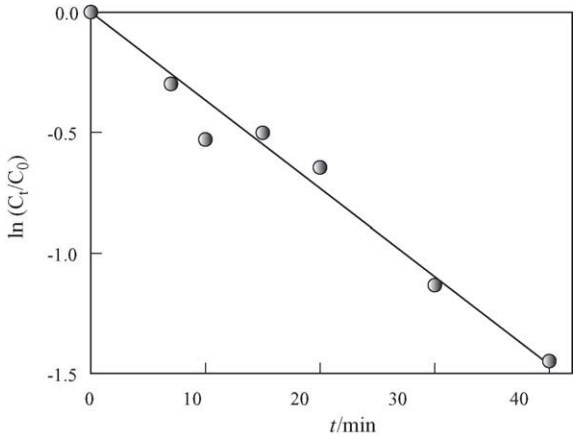

Fig. 7. First order kinetic plot for the heterogeneous photocatalytic degradation of catechol.

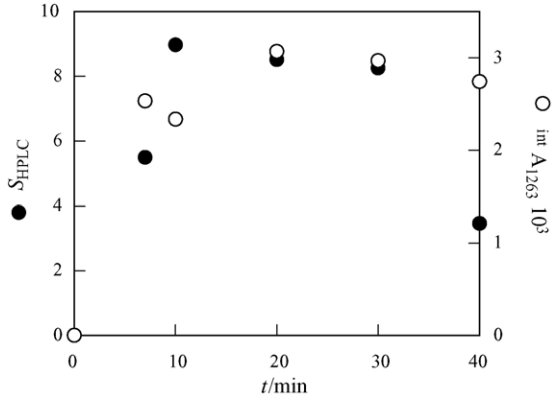

Fig. 8. Time evolution of the concentration of the reaction product eluting at 14.4 min, presented as the chromatogram signal intensity, and time evolution of the contribution from the intermediate to the band at 1263 cm^{-1} (see text).

which light intensity influence is only minor. Two important conclusions can be drawn for this second regime: (a) the rate of photolysis of the surface species is limited by the rate of provision of fresh ligand from the solution; (b) either the rate of photolysis of least stable species III and II is higher than that of species I, or that III and II evolve directly on the surface to I, when this last complex is depleted by photolysis. Further experiments shall probe into this matter.

In the case of catechol, the first order kinetics measured by HPLC (Fig. 7) is compatible with various possible rate limiting steps. Combination of FT-IR and HPLC data provides evidence that the reactive surface is not equilibrated with the bulk solution. Fig. 10 presents a plot of the intensity of the 1486 cm^{-1} peak (normalized with respect to that at full catechol coverage) as a function of the solution concentration measured by HPLC. The Langmuir isotherm derived from dark measurements is also shown. It is seen that the surface is largely depleted of catechol. This indicates that adsorp-

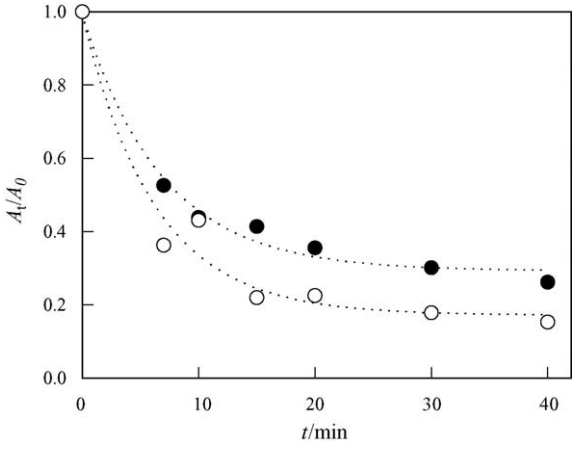

Fig. 9. Time evolution of the absorbance due to catechol surface complexes during UV-light illumination: (◯) 1486 cm^{-1}; (●) 1263 cm^{-1}; initial catechol concentration: 1.0×10^{-4} M; light intensity: 1.95×10^{-4} E cm^{-2}; pH 6.2; dotted lines are drawn for visual aid only.

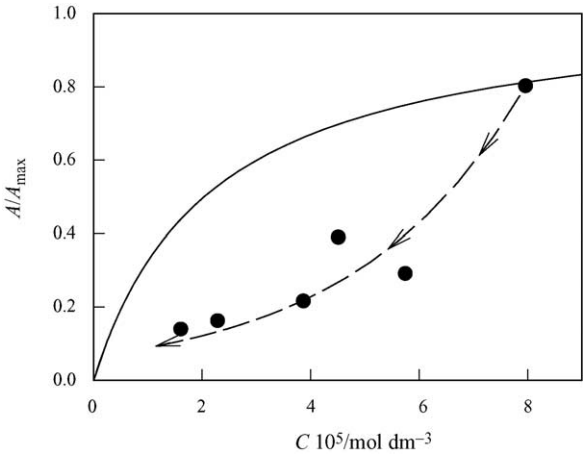

Fig. 10. Absorbance of the 1486 cm^{-1} band due to catechol surface complexes as a function of the remnant catechol concentration; the absorbance is normalized with respect to A_{max}, i.e., that corresponding to complete surface coverage. The full line represents the equilibrium, dark, adsorption isotherm. The arrows on the dashed line, drawn for visual aid, indicate the evolution of the degree of coverage during UV-light illumination.

tion of fresh reagent limits the rate. At long reaction times (20–40 min), a steady state degree of coverage, accounting for ca. 30% of the equilibrium coverage, is attained. The first order kinetics of Fig. 7 should therefore be attributed to kinetic control by the adsorption of the ligand. In agreement, Robert et al. [25], through DRIFT measurements, suggest that phenols chemisorb slowly onto TiO_2.

Photo-oxidation of oxalate shows only a modest influence of light intensity; again, this result indicates that the rate of photolysis is fast as compared to mass transfer.[4] Simple limiting kinetic cases were described in Ref. [18]. They apply to the following very simple kinetic scheme:

$$> \text{Ti–OH} + \text{HL} \underset{k_{-1}}{\overset{k_1}{\rightleftarrows}} > \text{Ti–L} + \text{H}_2\text{O} \quad (2)$$

$$> \text{Ti–L} + h^+ \xrightarrow{k_2} > \text{Ti–P}^+ \quad (3)$$

$$> \text{Ti–P}^+ + \text{H}_2\text{O} \underset{k_{-3}}{\overset{k_3}{\rightleftarrows}} > \text{Ti–OH} + \text{HP}^+ \quad (4)$$

Accepting that the fundamental process is the capture of a hole by the adsorbed ligand, the rate at the steady state is

$$R = k_2\{> \text{Ti–L}\}\{h^+\} = \frac{k_1 k_2 (N_S/Q)[\text{HL}]\{h^+\}}{k_{-1} + k_2\{h^+\}} \quad (5)$$

In this equation, R is the rate of the interfacial process; i.e., $-\text{d[HL]}/\text{d}t = (A_S w/V)\ R$, where w is the mass of TiO_2, A_S the specific surface area, and V is the solution volume. The kinetic constants k_1 ($M^{-1}\ s^{-1}$), k_{-1} (s^{-1}), k_2 ($mol^{-1}\ m^2\ s^{-1}$), k_3 (s^{-1}), and k_{-3} ($M^{-1}\ s^{-1}$) refer to the individual steps of the mechanism written above. {} denotes surface concentration in mol m^{-2}, $\{h^+\}$ is the effective number of holes defined by the light intensity, N_S (mol m^{-2}) is the number of available adsorption sites, and [HL] is the bulk concentration of the ligand. For oxidation products that bear very low affinity for the surface (i.e., $k_{-3}[\text{HP}^+]/k_3 \ll 1$), Q is given by (see Appendix A):

$$Q = 1 + \frac{k_1[\text{HL}]}{k_{-1} + k_2\{h^+\}} + \frac{k_1 k_2[\text{HL}]\{h^+\}}{k_3(k_{-1} + k_2\{h^+\})} \quad (6)$$

Depending on the relative values of the terms in Q, four limiting cases can be envisaged, with different dependencies on light intensity and substrate bulk concentration. They are:

(1) For low degrees of coverage, $Q \cong 1$, and slow photoreactions, $k_{-1} \gg k_2\{h^+\}$:

$$R = \frac{k_1 k_2 N_S[\text{HL}]\{h^+\}}{k_{-1}} \quad (7)$$

(2) For surface coverage dominated by equilibrated chemisorption, $Q = 1 + (k_1/k_{-1})$ [HL]. Thus, for slow photoreactions, $k_{-1} \gg k_2\{h^+\}$, and full ligand coverage:

$$R = k_2 N_S\{h^+\} \quad (8)$$

(3) For low degrees of coverage, $Q \cong 1$, determined by fast surface reactions, $k_2\{h^+\} \gg k_{-1}$:

$$R = k_1 N_S[\text{HL}] \quad (9)$$

(4) For slow desorption of the reaction product that covers most of the surface sites:

$$Q \cong \frac{k_1 k_2[\text{HL}]\{h^+\}}{k_3(k_{-1} + k_2\{h^+\})} \quad \text{and} \quad R = k_3 N_S \quad (10)$$

The behavior of catechol approaches limiting condition (3), although the steady state may be reached only in latter stages (cf. Figs. 9 and 10). In the case of oxalate, for the slower reaction established after ca. 2500 s, comparison of slopes at the two concentrations lead to an apparent kinetic order of one on bulk oxalate concentration, and a minor dependency on light intensity, suggesting again the system approaches the limiting behavior (3). In the early stages however, there is no steady state, and the behavior is complex.

5. Conclusions

ATR–FT-IR yields coherent and detailed information about the time evolution of the photocatalytic surface during illumination. Accumulation of intermediates and reaction products can be characterized, and the kinetic law, expressed in terms of surface concentrations can be derived. Comparison of this law with the conventional rate derived

[4] It is worth stressing that for experiments carried out under stagnant conditions, like those presented here, no clear-cut distinction between adsorption control and mass transfer control can be made. These terms are used here indistinctly to indicate that formation of >Ti–L surface complexes limits the rate of photo-oxidation. At the explored conditions, diffusion may probably determine the overall rate of chemisorption.

from solution measurements permits to evaluate the relative slowness of the photolytic step and of the mass transfer steps.

Acknowledgements

Work supported by the European Commission INCO Project *Cost Effective Solar Photocatalytic Technology to Water Decontamination and Disinfection in Rural Areas of Developing Countries (SOLWATER)* ICA4-CT-2002-10001, and Agencia Nacional de Promoción de Ciencia y Tecnología of Argentina (PICT 06-06631). This work is part of Program P-5 of Comisión Nacional de Energía Atómica. MAB, PJM and AER are members of the Research Career of CONICET. A doctoral fellowship by CONICET to C.B.M. is acknowledged.

Appendix A

Q in Eq. (5) quantifies the actual surface concentration of uncomplexed >Ti–OH sites, i.e., N_S/Q. Its value is determined by the interplay of the rate processes depicted by

$$> \text{Ti–OH} + \text{HL} \underset{k_{-1}}{\overset{k_1}{\rightleftarrows}} > \text{Ti–L} + \text{H}_2\text{O} \tag{A.1}$$

$$> \text{Ti–L} + h^+ \xrightarrow{k_2} > \text{Ti–P}^+ \tag{A.2}$$

$$> \text{Ti–P}^+ + \text{H}_2\text{O} \underset{k_{-3}}{\overset{k_3}{\rightleftarrows}} > \text{Ti–OH} + \text{HP}^+ \tag{A.3}$$

At the surface steady state, $\mathrm{d}\{>\text{Ti–OH}\}/\mathrm{d}t = \mathrm{d}\{>\text{Ti–L}\}/\mathrm{d}t = \mathrm{d}\{>\text{Ti–P}^+\}/\mathrm{d}t = 0$, and Eqs. (A.1)–(A.3) yield

$$\{> \text{Ti–L}\} = \frac{k_1\{> \text{Ti–OH}\}[\text{HL}]}{k_{-1} + k_2\{h^+\}} \tag{A.4}$$

$$\{> \text{Ti–P}^+\} = \frac{k_{-3}\{> \text{Ti–OH}\}[\text{HP}^+]}{k_3} + \frac{k_1 k_2\{> \text{Ti–OH}\}[\text{HL}]\{h^+\}}{k_3(k_{-1} + k_2\{h^+\})} \tag{A.5}$$

Replacing $\{>\text{Ti–L}\}$ and $\{>\text{Ti–P}^+\}$ in the surface mass balance:

$$N_S = \{> \text{Ti–OH}\} + \{> \text{Ti–L}\} + \{> \text{Ti–P}^+\} \tag{A.6}$$

one obtains

$$N_S = \{> \text{Ti–OH}\}\left(1 + \frac{k_1[\text{HL}]}{k_{-1} + k_2\{h^+\}} + \frac{k_{-3}[\text{HP}^+]}{k_3} + \frac{k_1 k_2[\text{HL}]\{h^+\}}{k_3(k_{-1} + k_2\{h^+\})}\right) = \{> \text{Ti–OH}\}Q \tag{A.7}$$

References

[1] Y. Arai, D.L. Sparks, J. Colloid Interface Sci. 241 (2001) 317.
[2] M.I. Tejedor-Tejedor, M. Anderson, Langmuir 6 (1990) 602.
[3] S.J. Hug, J. Colloid Interface Sci. 188 (1997) 415.
[4] S.J. Hug, B. Sulzberger, Langmuir 10 (1994) 3587.
[5] A.D. Weisz, A.E. Regazzoni, M.A. Blesa, Solid State Ionics 143 (2001) 125.
[6] A.D. Weisz, L. García Rodenas, P.J. Morando, A.E. Regazzoni, M.A. Blesa, Catal. Today 76 (2002) 103.
[7] M.A. Blesa, A.D. Weisz, P.J. Morando, J.A. Salfity, G.E. Magaz, A.E. Regazzoni, Coord. Chem. Rev. 196 (2000) 31.
[8] J.M. Kesselman-Truttmann, S.J. Hug, Environ. Sci. Technol. 33 (1999) 3171.
[9] P. Mandelbaum, A.E. Regazzoni, M.A. Blesa, S.A. Bilmes, J. Phys. Chem. 103 (1999) 5505.
[10] A.E. Regazzoni, P. Mandelbaum, M. Matsuyoshi, S. Schiller, S.A. Bilmes, M.A. Blesa, Langmuir 14 (1998) 868.
[11] P. Mandelbaum, S.A. Bilmes, A.E. Regazzoni, M.A. Blesa, Solar Energy 65 (1999) 75.
[12] J.M. Kesselman, N.S. Lewis, M.R. Hoffmann, Environ. Sci. Technol. 31 (1997) 2298.
[13] M.E. Calvo, R.J. Candal, S.A. Bilmes, Environ. Sci. Technol. 35 (2001) 4132.
[14] R. Rodríguez, M.A. Blesa, A.E. Regazzoni, J. Colloid Interface Sci. 177 (1996) 122.
[15] J.M. Kesselmann, O. Weres, N.S. Lewis, M.R. Hoffmann, J. Phys. Chem. B 101 (1997) 2637.
[16] S.T. Martin, J.M. Kesselmann, D.S. Park, N.S. Lewis, M.R. Hoffmann, Environ. Sci. Technol. 30 (1996) 2535.
[17] C.B. Mendive, A.D. Weisz, M.A. Blesa, Presented at the 11th International Conference on Surface and Colloid Science, September 15–19, Iguassu Falls, Brasil, 2003.
[18] M.A. Blesa, R.J. Candal, S.A. Bilmes, in: E. Matijević, M. Borkovec (Eds.), Surface and Colloid Science, 17, Kluwer, New York, 2004, pp. 83–111.
[19] E. Pelizzetti, C. Minero, Electrochim. Acta 38 (1993) 47.
[20] T. Ivanova, J.A. Harizanova, Solid State Ionics 138 (2001) 227.
[21] P.A. Connor, K.D. Dobson, A.J. McQuillan, Langmuir 15 (1999) 2402.
[22] J. Theurich, M. Linder, D.W. Bahnemann, Langmuir 12 (1996) 6368.
[23] A.M. Peiró, J.A. Ayllón, J. Peral, X. Doménech, Appl. Catal. B 30 (2001) 359.
[24] G.L. Puma, P.L. Yue, Ind. Eng. Chem. Res. 41 (2002) 5594.
[25] D. Robert, S. Parra, C. Pulgarin, A. Krzton, J.V. Weber, Appl. Surface Sci. 167 (2000) 51.